Optimal Drift Orbit Planning for a Multiple Space Debris Removal Mission using High-Accuracy Low-Thrust Transfers

Mikkel Jorgensen(1), Inna Sharf(2)

(1)Department of Mechanical Engineering, McGill University, 845 Sherbrooke St W, H3A 0G4, Montréal, Québec, Canada, mikkel.jorgensen@mail.mcgill.ca
(2)Department of Mechanical Engineering, McGill University, 845 Sherbrooke St W, H3A 0G4, Montréal, Québec, Canada, inna.sharf@mcgill.ca

Abstract

In this paper, we reduce the fuel cost of accurate rendezvous with multiple pieces of space debris in a single mission by introducing an optimized drift orbit for transfers requiring large changes in right ascension of the ascending node (RAAN). Continuous low thrust maneuvers are used to achieve each orbital transfer. The mission scenario considered requires the chaser to capture and de-orbit the debris into a disposal orbit, after which it releases the debris, performs a transfer and rendezvous with the next debris, continuing until the end of the mission in a recursive fashion. Within each rendezvous phase, the orbital drift of both the chaser and the target are considered. This is done in order to ensure the orbital elements of the chaser are matched to the actual location of the debris at the end of the maneuver. If the RAAN difference between the chaser and the debris is deemed large, a drift orbit is introduced during rendezvous. Each maneuver is defined as a minimum-time orbital transfer, and the transfer is posed as a constrained non-linear optimal control problem, implemented in GPOPS-II — a Matlab based software. The initial guess for the transfer time constitutes the period over which the given piece of debris is propagated to find the location of the debris after transfer. The location of the debris is then used as an initial guess for the final boundary constraint of the chaser's high-accuracy transfer. This procedure is iterated until the post-propagation location of the debris matches the location of the chaser following the high-accuracy transfer, within certain error bounds. A set of five debris with large RAAN differences situated in lower Earth orbit (LEO) have been selected for demonstrating the proposed methodology. The outcome is the best possible trade-off between time and fuel for the multiple-debris removal mission and the control inputs required to achieve it.

1. Introduction

As a consequence of the increasing utility of and reliance on satellites, lower Earth orbits have become the residence for a significant number of large space debris. Space debris is defined as objects in near-Earth space that have lost their functionality, are no longer under active control and/or have lost communication. These debris are at risk of colliding with working satellites or other debris, which results in a cascading effect of more debris being generated. Additionally, spacecraft launches into LEO are occurring at an increasing rate. As such, for the continued safe utilization of space capabilities in LEO, active debris removal (ADR) has become a topic of intense research for future space missions [1]. Large debris in particular, such as spent satellites or launchers stages, need to be removed from near-Earth space in order to carry out future space missions safely. Multiple debris missions are not only important from a financial perspective but also from a time efficiency perspective [1][2].

The category of multi-debris missions chosen for this research involves a chaser de-orbiting the targeted debris and then returning to another debris location in order to de-orbit the next piece of debris in a sequential fashion, as depicted in Figure 1a. In addition, a drift orbit is introduced during the rendezvous stage for each debris, as seen in Figure 1b, to compensate for significant RAAN differences between the chaser and the debris. As a result, the chaser performs an orbit to orbit transfer to reach the

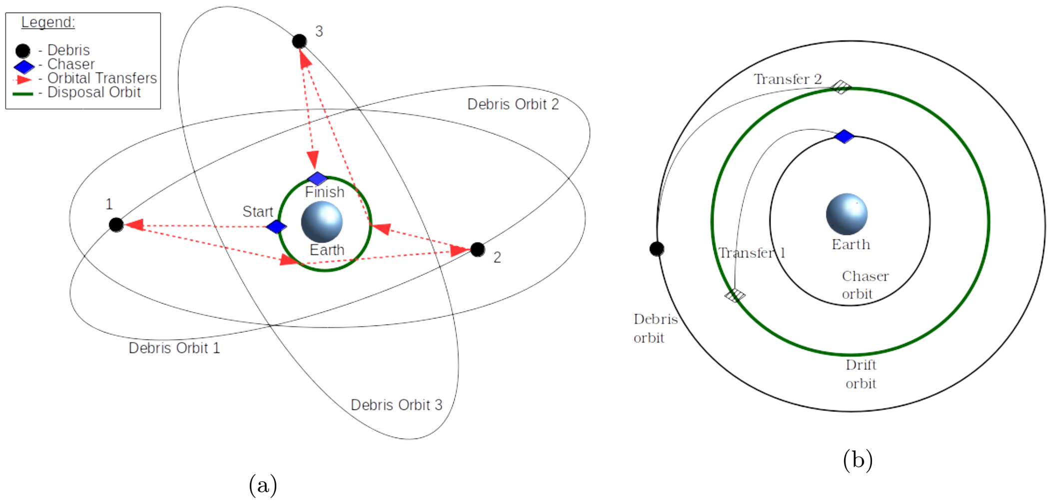

Figure 1: (a) Recursive multiple debris removal scenario for three debris (b) Rendezvous transfer with drift orbit

desired drift orbit, then drifts for a set amout of time to compensate for RAAN differences, and lastly performs a point-to-point transfer to achieve rendezvous with the debris. This approach is well suited for capture methods where the chaser must de-orbit the debris before returning to the next debris. This includes methods resulting in docking of the chaser and the debris, as well as those resulting in a tethered connection between the chaser and the debris, such as the tethered-net capture methods [3] or harpoon capture [4]. Furthermore, in the present paper, low-thrust maneuvers are chosen for the multiple debris removal mission as a way of minimizing fuel consumption.

The research presented in this paper focuses on applying low-thrust orbital dynamics to LEO transfers and more specifically on introducing a RAAN drift orbit while achieving rendezvous with large debris; the novelty here is the emphasis on removing debris with RAAN differences exceeding the RAAN change envelope of the chaser for a given transfer. Each transfer is carried out using low thrust maneuvers to achieve multiple ADR in a cost-efficient manner, while minimizing the time used to do so. First, the outline of the proposed approach is followed by the methodology defining the low-thrust dynamics, the introduction and selection of each drift orbit, and a presentation of the optimal control problem set-up to be solved in order to achieve optimized transfers. A brief explanation of how the problem is solved numerically is presented, followed by the results for one set of actual space debris, the data for which is obtained from TLEs [5]. The feasibility of achieving the RAAN changes required for given transfers is assessed and conclusions that can be drawn from this analysis are presented.

2. Equations of Motion of the Chaser and Drift Orbit Selection

Given the recursive scenario outlined in Figure 1a, a mission plan is required in which the ADR procedure can be evaluated and analyzed. The recursive scenario requires multiple orbital transfers, as the chaser needs to rendezvous with each debris and de-orbit them into the disposal orbit separately. In addition, to reduce the fuel cost required to compensate for large RAAN differences between the chaser and the various pieces of debris, an optimized drift orbit is introduced during rendezvous, as shown in Figure 1b. As a result, the chaser performs an orbit-to-orbit transfer from the original parking or disposal orbit to the drift orbit, after which it is left to drift within the drift orbit, and finally it performs an accurate point-to-point transfer from the drift orbit to the debris location. An appropriately chosen drift orbit allows the chaser RAAN to 'catch up' with the debris RAAN at the expense of time rather than fuel.

The section provides the methodology used for calculating the costs associated with high accuracy rendezvous with a drift orbit and de-orbiting of space debris in LEO, in terms of time and fuel. For the purpose of this research, the chaser spacecraft is modeled as a point mass with constant continuous low-thrust that can be applied in an arbitrary variable direction. As acknowledged by other authors [6][7], the attraction of a low-thrust propulsion system is the payload efficiency, i.e., lower amount of fuel mass

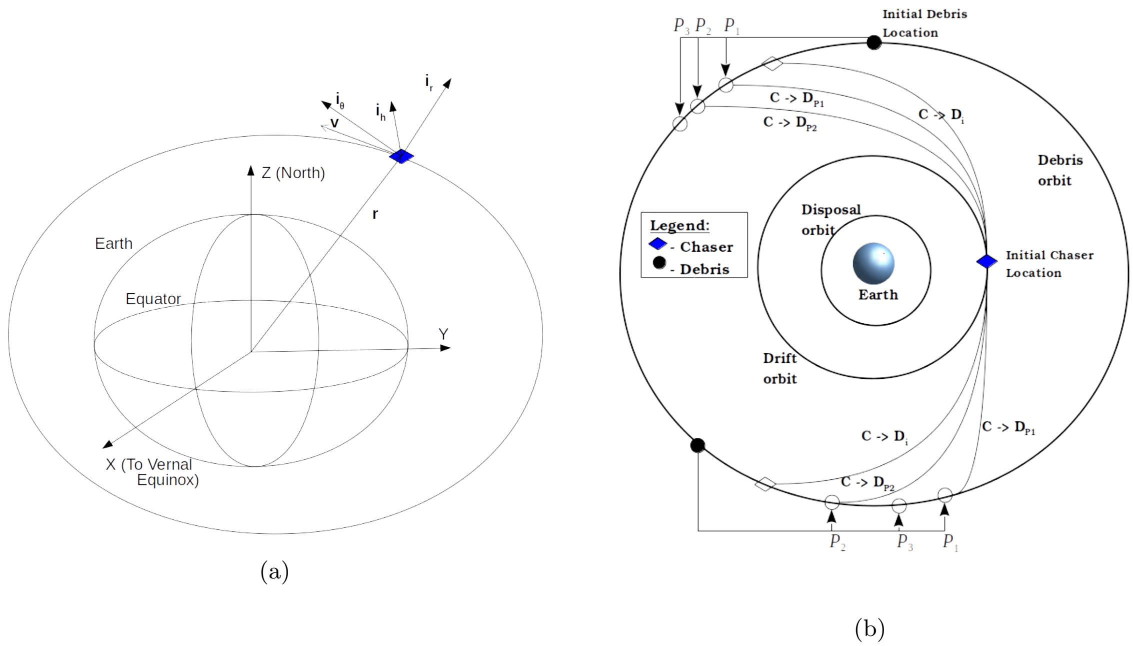

Figure 2: (a) Earth-centered inertial frame $[X\ Y\ Z]$ and rotating radial frame $[\mathbf{i}_r\ \mathbf{i}_\theta\ \mathbf{i}_h]$ (b) Illustration of Iterative Rendezvous Process from Drift Orbit to Debris

needed for a given ΔV requirement. In addtion, the D-SPOSE tool [8] is used to propagate the chaser during drift and the debris throughout the mission, applying only gravitational perturbations.

Two main reference frames are used throughout this research to describe the motion of the debris and the chaser. The first reference frame is the Earth-centered inertial (ECI) frame, defined by the X-Y-Z axes in Figure 2a, and the other is the rotating radial frame, local to the chaser, defined by the $[\mathbf{i_r}, \mathbf{i}_\theta, \mathbf{i_h}]$ unit vectors, as shown in Figure 2a.

2.1. Chaser equations of motion

Providing active debris removal in LEO requires accurate rendezvous between the chaser spacecraft and the debris. In order to achieve such a transfer, the optimal thrust directions, described in rotating radial coordinates as (u_r, u_θ, u_h), which minimize the time taken for a spacecraft to move from one point in space (defined by orbital elements) to another must be identified. The orbital elements are defined as semi-major axis (a), eccentricity (e), inclination (I), right-ascension-of-the-ascending-node (RAAN, Ω), argument of perigee (ω), and true anomaly (θ).

In this work, the dynamics of the spacecraft are propagated using modified equinoctial elements (p, f, g, h, k, L) [9],[10] where p is the semi-latus rectum, f and g are elements that describe the eccentricity, h and k are elements that describe the inclination, and L is the true longitude. The state of the spacecraft is converted from orbital elements to modified equinoctial elements to avoid numerical singularities associated with zero eccentricity and/or 90° inclination [11]. The modified equinoctial elements can be found from the orbital elements using the following standard equations:

$$\begin{aligned} p = a(1-e^2), \quad f = e\cos(\omega+\Omega), \quad g = e\sin(\omega+\Omega), \\ h = \tan(0.5I)\sin(\Omega), \quad k = \tan(0.5I)\cos(\Omega), \quad L = \Omega+\omega+\theta \end{aligned} \tag{1}$$

The differential equations of motion of the spacecraft and the derivation thereof can be found in [10]. It is important to note that the dynamics of the semi-major axis, inclination, and RAAN are coupled, making the problem of accurate point-to-point transfers non-trivial. The chaser acceleration components described in the rotating radial frame as Δ_r, Δ_θ, and Δ_h arise due to the thrust accelerating the chaser itself, as well as the perturbations affecting the spacecraft. The chaser acceleration is modeled as

$$\mathbf{\Delta} = \mathbf{\Delta}_g + \mathbf{\Delta}_T \tag{2}$$

where $\mathbf{\Delta}_g$ is the gravitational acceleration and $\mathbf{\Delta}_T$ is the thrust specific force. The definition of the gravitational acceleration term can be found in [12] and the thrust specific force is given as

$$\mathbf{\Delta}_T = \frac{T}{m}\mathbf{u} \tag{3}$$

where

$$\mathbf{u} = (u_r, u_\theta, u_h) \tag{4}$$

represents the thrust direction and is a unit vector, m is the mass of the chaser, and T is the continuous thrust value.

2.2. Drift Orbit Selection

In this section, an optimization procedure for selecting a drift orbit for a given debris rendezvous is formulated based on previous work by the authors [13]. Here, the aim is to find the drift orbit for which the overall transfer time for rendezvous (time for transfer 1 and transfer 2 in Figure 1b, as well as drift time) is minimized.

To begin, the limit on the RAAN change that can be achieved by the chaser, given the required altitude and inclination changes for the transfer, needs to be identified in order to determine whether a drift orbit is necessary. This limit can be estimated. First by considering the natural RAAN changes caused by Earth oblateness, which contribute to the overall RAAN changes during transfers and propagations. Second, there is a limit on the RAAN change that can be provided by the chaser thrusters within a given altitude and/or inclination change. This means there is not only a maximum RAAN change for a given transfer or propagation, but also a minimum, the resulting envelope specified by:

$$\Delta\Omega_{envelope} = \Delta\Omega_{perturb} \pm \Delta\Omega_{thrust} \tag{5}$$

The well-known relationship for the rate of change of RAAN due to Earth oblateness is given by:

$$\dot{\Omega}_{perturb}(t) = -\frac{3}{2}J_2\sqrt{\mu}R_e^2 a(t)^{-7/2}\cos I(t) \tag{6}$$

In addition, the maximum $\Delta\Omega_{thrust}$ can be estimated by assuming optimal thrust directions for altitude and RAAN changes throughout the orbital transfer. These optimal thrust directions can be found analytically [14], and the rate of change of RAAN due to thrust is given by:

$$\dot{\Omega}_{thrust}(t) = \frac{a\sin\theta}{H\sin I}u_h \tag{7}$$

where $H = \sqrt{\mu p}$ is the magnitude of the angular momentum of the orbit. Eq. 7 is the general equation for RAAN change for thrust direction u_h, which maximizes RAAN and altitude change when $u_h = \frac{T}{wg_e}\sin\beta^*$ with β^* the optimal yaw angle for said change, given by:

$$\beta^* = \text{sign}(\sin\theta)\frac{\pi}{4} \tag{8}$$

The $\Delta\Omega_{envelope}$ for a given transfer can then be estimated by integrating Eqs. (6) and (7) over the time of transfer, estimated using Edelbaum's low-thrust transfer analysis [6].

Next, considering Eq. (6), the natural drift rate is inversely proportional to the altitude of the orbit. This means the drift orbit should be at as low an altitude as possible, while ensuring that the aerodynamic drag does not cause significant perturbations to the drift orbit parameters during drift. A conservative estimate obtained using the D-SPOSE tool [8] of the decay rate at an altitude of 500 km is 0.14 km/day, which is deemed sufficiently low for the purpose of the drift orbits.

Finally, the inclination of the drift orbit is determined by minimizing the overall rendezvous time:

$$\begin{aligned} \min_{I_{drift}} \quad & f(I_{drift}) = t_{transfer1} + t_{transfer2} + t_{drift} \\ \text{subject to} \quad & g_1(I_{drift}) = \Delta V_{a,I} - \Delta V_{max} \leq 0 \\ & g_2(I_{drift}) = t_{total} - t_{max} \leq 0 \end{aligned} \tag{9}$$

where $\Delta V_{a,I}$ is the sum of the total transfer ΔV for transfers 1 and 2, given that the drift drift stage does not require ΔV and accounts for any ΔV required to match the debris RAAN; ΔV_{max} is the ΔV estimate for performing the rendezvous without a drift orbit; t_{total} is the sum of the total transfer time taken to rendezvous with the debris ($t_{transfer1} + t_{transfer2} + t_{drift}$) as shown in Figure 1b, and t_{max} is the maximum allowable time for the transfer. The parameters t_{max} and ΔV_{max} are constant for a given transfer, and t_{max} is user defined. The value for $t_{transfer}$ and $\Delta V_{a,I}$ for both orbital maneuvers during rendezvous are calculated using Edelbaum's equations for low-thrust orbit-to-orbit transfers [6]. The estimate for t_{drift} is calculated by comparing the drift rate of a given drift orbit, Eq. (6) to the drift rate of a given piece of debris and finding the time taken for the chaser RAAN to 'catch up' to the debris RAAN, while accounting for the RAAN changes that will occur during transfer 2 (after the drift).

3. Optimized Solution for Point-to-Point Transfer

To achieve a rendezvous between the chaser and the debris sufficient for ADR, a high accuracy point-to-point transfer is required. It is therefore important to take into account the changes in true anomaly as well as the other orbital elements, not usually required during other missions where low thrust is used [15]. The aim of the optimization formulation presented here is to achieve such a high accuracy transfer in LEO and to determine the trajectory and the control directions which minimize the following objective function:

$$J = t_{transfer2} \tag{10}$$

for a chaser with the state, $\mathbf{x}$

$$\mathbf{x} = (p, f, g, h, k, L, w) \tag{11}$$

subject to the dynamics described in Section 2.1. Transfer time for the point-to-point transfer (transfer 2) is chosen as the minimization objective due to the continuous thrust nature of the transfer: if the thrust is constant and continuous, the shortest transfer time is also the most fuel efficient.

3.1. Boundary Conditions and Path Constraint

The boundary conditions for the orbit transfer are described in terms of classical orbital elements and converted to modified equinoctial elements using Eq. (1). The chaser starts in a near-circular inclined low Earth orbit, and the initial debris location is given by two-line-elements [5] data at time $t_0 = 0$. The initial orbit, in this case the drift orbit, is specified in terms of classical orbital elements as

$$[a(t_0)\ \ e(t_0)\ \ I(t_0)\ \ \Omega(t_0)\ \ \omega(t_0)\ \ \theta(t_0)] = [a_0\ \ e_0\ \ I_0\ \ \Omega_0\ \ \omega_0\ \ \theta_0] \tag{12}$$

The orbital transfer of the chaser is terminated at the debris location after propagation, given by

$$[a(t_f)\ \ e(t_f)\ \ I(t_f)\ \ \Omega(t_f)\ \ \omega(t_f)\ \ \theta(t_f)] = [a_f\ \ e_f\ \ I_f\ \ \Omega_f\ \ \omega_f\ \ \theta_f] \tag{13}$$

Finally, during the transfer, the thrust direction $\mathbf{u}$ must remain a unit vector. Thus, the equality path constraint given by Eq. (14) is implemented at all points during the transfer.

$$||\mathbf{u}||_2 = u_r^2 + u_\theta^2 + u_h^2 = 1 \tag{14}$$

3.2. Solving Optimal Control Problem

The minimum-time low-thrust optimal control problem analyzed here is solved using the optimal control software GPOPS-II [16]. GPOPS-II is a MATLAB software that transcribes an optimal control problem to a nonlinear programming problem (NLP) on a given mesh. In order to do this, GPOPS-II implements the variable-order LegendreGaussRadau (LGR) quadrature collocation method [17], together with an hp-adaptive mesh refinement method [18]. The NLP arising from the LGR collocation method is solved using the open-source NLP solver IPOPT (interior point optimizer) [19], which implements a primal-dual interior point method [20]. Analytical first and second derivatives are obtained using the open-source algorithmic differentiation package ADiGator, for which the underlying algorithm is described in [21].

3.2.1. Iterative Solution

To achieve a high accuracy transfer, it is necessary to match the chaser's arrival location to the actual location of the debris after the transfer time. This means the location of the debris needs to be propagated for the duration of the estimated transfer time, and a new transfer problem needs to be solved for the new debris location. This applies only to transfer 2 (drift orbit to debris location), and the process is illustrated in Figure 2b. Given that the chaser is transferred to an estimated debris location, an iterative procedure is required in order to achieve convergence between the final chaser location and the actual debris location after transfer. By propagating the debris orbital elements for the duration of the rendezvous found using the D-SPOSE orbital propagator, a more accurate location of the debris can be found, and the optimal control problem for transfer 2 can be solved again for the updated debris location. The iterations are repeated until the chaser location after the transfer matches the propagated debris location after said chaser transfer time. This iterative procedure is illustrated in Figure 2b, where an optimal control problem is solved, in which the chaser is transferred to the initial debris orbit ($C \rightarrow D_i$) in t_c^0 days. The debris is then propagated (P_1) for duration t_c^0, and a new debris location is found. The chaser is transferred to new debris location ($C \rightarrow D_{P_1}$), and a new transfer time t_c^1 is found. The debris is then propagated (P_2) for t_c^1 days, and a corresponding transfer time to this next location is calculated. This process is repeated until the difference in sequential propagation times, $t_c^n - t_c^{n-1}$, is smaller than a desired specified tolerance.

The iterative procedure described above is initiated by specifying each debris location only at the beginning of the mission. This means consecutive debris in the multiple debris removal mission are propagated from the beginning of the mission, over the time taken to remove previous debris, through to the rendezvous with the debris at hand. However, the chaser transfer time is only considered as the time from the moment the chaser and the previous debris have arrived in the disposal orbit, to the time of rendezvous between the chaser and the current debris.

4. Results and Discussion

4.1. Mission Parameters

For the results presented in this paper, the mass of the chaser is assumed to be 2000 kg [22], as this is an adequate mass for removing large debris. In addition, approximately 50% of the total chaser mass is assumed to be fuel, which is a feasible requirement for long range space missions [23]. For the continuous thrust maneuvers, the thrust T of the chaser is taken as 0.5 N, and the specific impulse, needed to estimate the fuel mass required for a given transfer, is chosen to be 2000 s [24]. The initial orbit of the chaser and the disposal orbit are only constrained to have an altitude of 200 km, as this is both a realistic parking orbit and the decay rate of debris at this altitude is reduced from an order of hundreds of years to within one year, i.e., the decay rate of the debris is high enough for it to burn up or enter the Earth's atmosphere without creating a significant collision risk.

For completing an iteration of the procedure presented in Section 3.2.1, we assume reasonable and practical constraints on the accuracy of matching the orbital elements of the chaser and the debris, as well as the time difference between the chaser after transfer and the debris post-propagation. In particular, each iteration is only complete if orbital elements of the chaser match those of the debris to within the following accuracies:

$$\begin{aligned} a_f &= a_d \pm 0.5 \text{ km}, \quad & e_f &= e_d \pm 0.001, \quad & I_f &= I_d \pm 0.01^\circ, \\ \Omega_f &= \Omega_d \pm 0.1^\circ, \quad & \theta_f &= \theta_d \pm 1^\circ, \quad & t_c^n - t_c^{n-1} &\leq 0.003 \text{ days} \end{aligned} \tag{15}$$

The 0.5 km semi-major axis tolerence specified in Eq. (15) is deemed an adequate distance for initiating close range rendezvous [25]. The other orbital elements margins were chosen based on attainability with current propulsion capabilities, while accounting for perturbations. No constraints are placed on the final argument of perigee $\omega(t_f)$, as the debris are all located in near-circular orbit. As noted earlier, the drift orbits are set at an altitude of 500 km due to the limited effect of atmospheric drag at this altitude for the purpose of this mission. Satisfying the RAAN and the time constraints proved the most difficult: the RAAN constraint because the time spent in drift orbit requires knowledge of the final RAAN of the debris as well as the RAAN change experienced by the chaser during transfer 2. The time constraint is only satisfied if the chaser and debris have the same location at approximately the same time, therefore relies on all the other constraints being satisfied as well.

4.2. Debris Selection

The debris of interest for the research in this paper are large defunct satellites and rocket stages with high risk factors [2]. The initial locations defined using orbital elements of the debris are shown in Table 1. The debris altitudes and inclinations are all in a narrow band around 760 km and 98°, however, the RAAN differences are very large for these debris. Moreover, this particular set of debris have very large masses, which will effect the de-orbiting stage of the debris removal mission. The sequence of the debris is chosen such that consecutive RAAN differences are as low as possible. Other than this, the particular debris choice and sequencing have not been optimized in any way to the specific ADR mission presented here. It is important to note that this set of debris was chosen for the purpose of showcasing the solution for the drift orbit within the context of high-accuracy transfers, and it does not necessarily represent a feasible mission. The mission start date is chosen to be 01-01-2016, such that historical data (TLEs and atmospheric density) can be used for simulation purposes.

Name	Norad ID	a (km)	e	I (deg)	Ω (deg)	ω (deg)	θ (deg)	approx. mass (kg)
Chaser	N/A	6578	0.0000	98.00	320.0	0.000	0.000	2000
Debris 1	25400	7185	0.0011	98.41	323.3	57.96	302.2	8226
Debris 2	28931	7065	0.0001	97.91	47.76	133.3	226.8	4000
Debris 3	27386	7144	0.0001	98.31	60.30	82.82	277.3	8111
Debris 4	27601	7164	0.0073	98.44	80.20	72.97	36.14	4000
Debris 5	27006	7374	0.0014	99.23	154.9	259.7	226.2	9000

Table 1: Debris and chaser initial locations

4.3. Analysis of Results

A summary of the results for the removal of the 5 debris set can be found in Table 2. Each line in the table represents a given stage in the proposed methodology. When propagating debris other than the first one in the sequence, the time taken to rendezvous and de-orbit previous debris also needs to be taken into account, and the propagation time for the debris is therefore cumulative and does not correspond to the chaser transfer time to that debris. Thus, for example, the time indicated in Table 2 for Deb.2 P_3 is the time taken to remove debris 1, in addition to the time for the chaser to transfer to the second drift orbit, drift, and then transfer to Deb.2 P_3. As a result, the later the debris appears in the five debris sequence, the longer it will be propagated. It should also be noted that the chaser is assumed to embark on each consecutive rendezvous immediately after the previous debris is de-orbited. The de-orbit results are calculated using the same methodology as the rendezvous, except only with a constraint on semi-major axis and all the other orbital elements left 'free' for the final disposal orbit. The time taken to de-orbit is long due to the combined mass of the debris and the chaser.

As the rendezvous with each debris is of similar nature, a closer look at the specific results for one debris (Figures 3 and 4) is adequate to provide insights into the chaser transfer response and control inputs of the full set. The three plots in Figure 3 show the progression of semi-major axis, inclination, and RAAN respectively over the course of the rendezvous for both the chaser and Debris 2; as can be seen, the orbital elements of the chaser reach the desired (debris) values at the end of the transfer. It should be noted that the importance of the drift orbit can be observed in the RAAN plot as the drift portion of the transfer allows for significant RAAN 'catch up'. There are oscillations in each of the variables, and these occur due to the perturbing effects of the Earth's oblateness. The control direction components (u_r, u_θ, u_h) for the point-to-point transfer (transfer 2) are shown in Figure 4. Changes in inclination occur throughout the transfer which is reflected in the oscillations in u_h, as well as the irregularities in u_r and u_θ. u_h oscillates between -1 and 1 to change angle of inclination in the appropriate direction depending on the location of the chaser within the transfer orbit, the u_h plot shown is only a section of the transfer to better highlight these results. This means, to decrease the inclination, u_h is most positive near apoapsis and most negative near periapsis. Moreover, the radial component oscillates around 0, as no change in eccentricity is required. The θ-component oscillates between 0 and 1. This signifies a focus on changing the semi-major axis while still achieving the desired inclination change. It should be noted that the majority of the RAAN change results from perturbations and not the thrust provided by the chaser shown by the RAAN limitation analysis described in Section 2.2. The large amplitude of oscillations of the control inputs is a

Transfer Description	a (km)	e	I (deg)	Ω (deg)	ω (deg)	θ (deg)	Time (days)	Fuel Mass (kg)
Chaser to drift 1	6877.6	0.0006	98.64	331.7	144.6	355.9	9.762	42.99
Drift 1	6885.2	0.0016	98.63	332.4	172.7	12.67	0.600	0.000
Deb. 1 P_1	7169.2	0.0008	98.43	341.0	328.3	140.3	18.39	N/A
Drift 1 to Deb. 1 P_1	7168.8	0.0003	98.44	341.0	29.54	139.3	8.030	35.60
Chaser and deb.1 de-orbit	6578.5	0.0002	98.42	61.60	123.8	46.27	77.74	344.6
Deb 1 Total	N/A	N/A	N/A	N/A	N/A	N/A	96.13	423.2
Chaser to drift 2	6878.5	0.0033	102.8	129.1	118.8	170.0	42.87	188.8
Drift 2	6883.7	0.0007	102.8	246.8	112.7	196.1	70.12	0.000
Deb. 2 P_3	7058.8	0.0022	97.91	292.4	129.6	264.6	254.7	N/A
Drift 2 to Deb.2 P_3	7058.4	0.0030	97.90	292.3	214.4	263.6	45.55	200.6
Chaser and deb.2 de-orbit	6574.8	0.0038	97.92	331.7	71.95	267.0	36.17	159.3
Deb.2 Total	N/A	N/A	N/A	N/A	N/A	N/A	194.7	548.7
Chaser to drift 3	6878.2	0.0040	99.74	0.004	14.32	162.4	21.36	94.04
Drift 3	6850.0	0.0059	99.74	10.62	53.92	161.8	8.043	0.000
Deb. 3 P_2	7133.8	0.0084	98.31	30.75	16.54	211.3	340.7	N/A
Drift 3 to Deb.3 P_2	7133.5	0.0082	98.31	30.76	11.08	241.7	20.42	89.93
Chaser and deb.3 de-orbit	6578.5	0.0029	98.32	142.6	34.58	234.7	114.1	502.3
Deb.3 Total	N/A	N/A	N/A	N/A	N/A	N/A	163.9	686.3
Chaser to drift 4	6879.1	0.0022	99.18	159.3	327.5	258.8	13.95	61.43
Drift 4	6871.0	0.0028	99.19	218.9	146.4	291.1	49.00	0.000
Deb. 4 P_2	7169.7	0.0052	98.46	232.5	308.5	120.3	532.6	N/A
Drift 4 to Deb.4 P_2	7169.4	0.0043	98.46	232.4	72.60	119.3	12.58	55.40
Chaser and deb.4 de-orbit	6578.5	0.0041	98.46	275.7	167.5	310.7	43.40	191.1
Deb.4 Total	N/A	N/A	N/A	N/A	N/A	N/A	118.9	307.9
Chaser to drift 5	6880.0	0.0051	102.6	339.8	33.63	78.15	45.64	201.0
Drift 5	6886.4	0.0032	102.6	59.32	271.6	314.6	48.10	0.000
Deb. 5 P_3	7385.1	0.0024	99.23	112.7	178.9	12.45	707.6	N/A
Drift 5 to Deb.5 P_3	7384.7	0.0018	99.24	112.5	21.98	12.38	37.24	166.6
Chaser and deb.5 de-orbit	6578.9	0.0016	99.24	215.0	236.3	74.35	106.0	466.9
Deb.5 Total	N/A	N/A	N/A	N/A	N/A	N/A	237.0	834.4
Mission Total:	N/A	N/A	N/A	N/A	N/A	N/A	813.6	2800.5

Table 2: Rendezvous transfer results summary — each line of data corresponds to the end of transfer described on that line

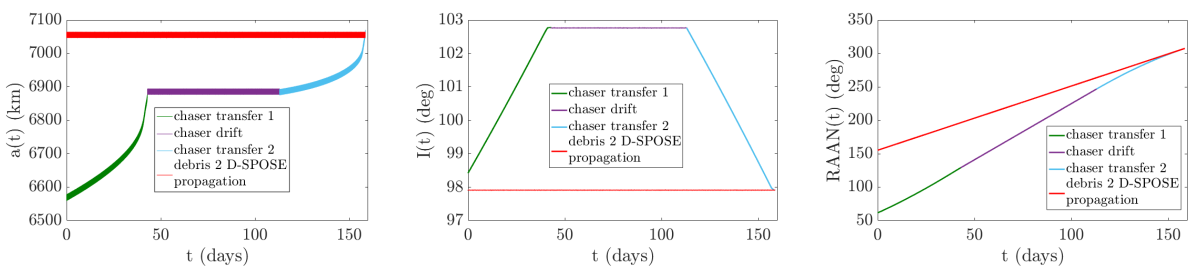

Figure 3: Main orbital elements during rendezvous with debris 2

representation of the change in thrust direction required to optimize out-of-plane changes such as inclination and RAAN, during orbital transfers requiring multiple revolutions. The smaller oscillations compensate for small perturbations arising due to Earth oblateness during the orbital transfer.

For the debris considered in this scenario, the most significant contributor to rendezvous transfer time is the change in RAAN, as we are focusing on debris with large RAAN differences. The large RAAN changes required result in higher inclination drift orbits, as a higher inclination (in the band around 98°) results in a higher drift rate, which also contributes to the time of transfer. The total time for rendezvous with and de-orbiting five pieces of debris is found to be 813.6 days. It is important to note that some time needs to be allocated for other aspects of a multi-debris removal mission, such as close-range rendezvous and capture of the debris, as well as releasing the debris. These results suggest that a full five-debris removal mission with massive debris in orbits with large differences in RAAN is not achievable within one-year time frame. It should also be noted that a main contributor to mission time is the long de-orbit time, due to the large masses of the debris showcased in this paper. Furthermore, de-orbiting all five debris requires significantly more fuel than is reasonable for a 2000 kg chaser. There are options for meeting a strict one-year time limit, and reducing the fuel cost for a five-debris removal mission, such as, selecting debris with lower masses (for example SL-8 rocket bodies have mass of ∼1440 kg) or by only having one or two debris with RAAN differences exceeding the RAAN envelope of the chaser (such as debris 1 and 2 — de-orbited in 290.8 days with 971.9 kg of fuel) , given that there is a large pool of debris to chose from.

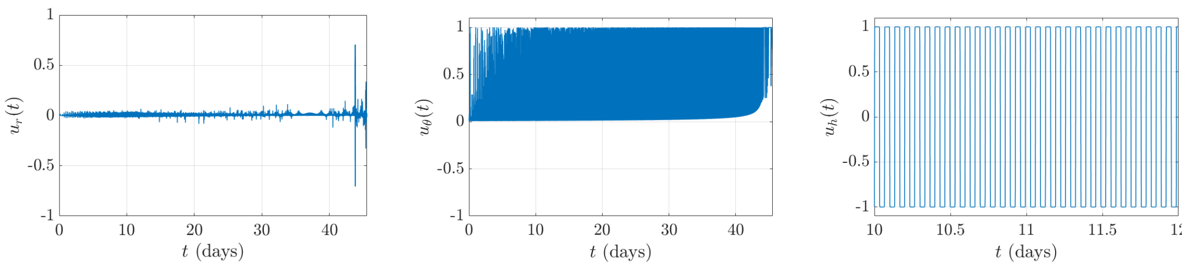

Figure 4: Chaser control direction components during transfer 2 of the rendezvous with debris 2

5. Conclusions

Removing multiple pieces of space debris from lower Earth orbit is required in order to remediate the LEO space environment and reduce the risk of collisions between space debris and active satellites. An approach suitable for multiple space debris removal, where the capture method results in a flexible connection between the chaser and the debris, is presented and analyzed in this paper. This approach requires each debris to be de-orbited before moving on to the next one. De-orbiting one debris before moving on to the next has proven costly, in terms of fuel cost. Therefore, each orbital transfer is performed assuming low continuous thrust and a point mass chaser. Moreover, the emphasis in this paper is on the rendezvous phase consisting of a transfer from the initial chaser orbit to an optimized drift orbit, and another transfer from the drift orbit to the debris location. A drift orbit is included to reduce the fuel cost due to large changes in RAAN required for high accuracy rendezvous between the chaser and the debris. During the final rendezvous stage, the chaser achieves an optimized high accuracy point-to-point transfer to the desired debris. The de-orbiting phases are optimized orbit-to-orbit transfers, as the position of release within the disposal orbit is assumed arbitrary. One set of five debris with large RAAN differences are considered in this paper. De-orbiting this particular set is deemed achievable within 2.23 years, with the main contributor to the time of transfer being the RAAN drift requirement and the long de-orbiting time due to the large mass of the debris.

The optimization procedure developed in this paper gives an accurate estimation of the time and fuel requirements for multi-debris removal missions even when the RAAN changes required exceed the RAAN change envelope of the chaser. Accomplishing these transfers without a drift orbit would make these missions unrealistic in terms of fuel required to match the debris RAAN, even for just one debris. Furthermore, the procedure takes true anomaly as well as perturbation effects in LEO into account, making it suitable for multiple space debris removal mission planning.

References

[1] J. Liou, A parametric study on using active debris removal for leo environment remediation, Adv Space Res 47 (11) (2011) 1865–1876.

[2] N. Van der Pas, J. Lousada, C. Terhes, M. Bernabeu, W. Bauer, Target selection and comparison of mission design for space debris removal by dlr's advanced study group, Acta Astronautica 102 (2014) 241–248.

[3] M. Shan, J. Guo, E. Gill, Deployment dynamics of tethered-net for space debris removal, Acta Astronautica 132 (2017) 293–302.

[4] R. Dudziak, S. Tuttle, S. Barraclough, Harpoon technology development for the active removal of space debris, Advances in Space Research 56 (3) (2015) 509–527.

[5] JSpOC, Two-line elements, website: `https://www.space-track.org/auth/login`, accessed: [Oct. 11, 2016]. (September 2016).
URL `https://www.space-track.org/auth/login`

[6] T. N. Edelbaum, Optimum low-thrust rendezvous and station keeping, AIAA Journal 2 (7) (1964) 1196–1201.

[7] J. T. Betts, Very low-thrust trajectory optimization using a direct sqp method, Journal of Computational and Applied Mathematics 120 (1) (2000) 27–40.

[8] S. L, Modeling and simulation of long-term rotational dynamics of large space debris, Ph.D. thesis, McGill University (2018).

[9] R. Brouke, P. Cefola, On the equinoctial orbital elements, Celestial Mechanics 5 (1972) 303–310.

[10] M. Walker, B. Ireland, J. Owens, A set modified equinoctial orbit elements, Celestial mechanics 36 (4) (1985) 409–419.

[11] J. T. Betts, Practical methods for optimal control and estimation using nonlinear programming, Vol. 19, Siam, 2010.

[12] K. F. Graham, A. V. Rao, Minimum-time trajectory optimization of multiple revolution low-thrust earth-orbit transfers, Journal of Spacecraft and Rockets 52 (3) (2015) 711–727.

[13] M. K. Jorgensen, I. Sharf, Planning and optimization for a multiple space debris removal mission, in: 2018 IEEE Aerospace Conference, IEEE, 2018.

[14] A. E. Petropoulos, Simple control laws for low-thrust orbit transfers (2003).

[15] A. Petropoulos, Low-thrust orbit transfers using candidate lyapunov functions with a mechanism for coasting, in: AIAA/AAS Astrodynamics Specialist Conference and Exhibit, 2004, p. 5089.

[16] M. A. Patterson, A. V. Rao, Gpops-ii: A matlab software for solving multiple-phase optimal control problems using hp-adaptive gaussian quadrature collocation methods and sparse nonlinear programming, ACM Transactions on Mathematical Software (TOMS) 41 (1) (2014) 1.

[17] D. Garg, M. Patterson, W. W. Hager, A. V. Rao, D. A. Benson, G. T. Huntington, A unified framework for the numerical solution of optimal control problems using pseudospectral methods, Automatica 46 (11) (2010) 1843–1851.

[18] C. L. Darby, W. W. Hager, A. V. Rao, An hp-adaptive pseudospectral method for solving optimal control problems, Optimal Control Applications and Methods 32 (4) (2011) 476–502.

[19] A. Waechter, C. Laird, F. Margot, Y. Kawajir, Introduction to ipopt: A tutorial for downloading, installing, and using ipopt, Revision (2009).

[20] R. Fletcher, S. Leyffer, P. L. Toint, et al., A brief history of filter methods, Preprint ANL/MCS-P1372-0906, Argonne National Laboratory, Mathematics and Computer Science Division (2006) 36.

[21] M. J. Weinstein, A. V. Rao, Algorithm 984: Adigator, a toolbox for the algorithmic differentiation of mathematical functions in matlab using source transformation via operator overloading, ACM Transactions on Mathematical Software (TOMS) 44 (2) (2017) 21.

[22] H. Linskens, E. Mooij, Tether dynamics analysis and guidance and control design for active space-debris removal, Journal of Guidance, Control, and Dynamics 39 (2016) 1232–1243.

[23] J. E. Graf, R. W. Zurek, H. J. Eisen, B. Jai, M. Johnston, R. Depaula, The mars reconnaissance orbiter mission, Acta Astronautica 57 (2-8) (2005) 566–578.

[24] Airbus, Ion propulsion systems, website: `http://www.space-propulsion.com/spacecraft-propulsion/ion-propulsion/index.html`, accessed: [March. 18, 2017]. (2003).

[25] L. Singh, S. Bortolami, L. Page, Optimal guidance and thruster control in orbital approach and rendezvous for docking using model predictive control, in: AIAA Guidance, Navigation, and Control Conference, 2010, p. 7754.